Applied Thermal Engineering 247 (2024) 123024

Contents lists available at ScienceDirect

Applied Thermal Engineering

journal homepage: www.elsevier.com/locate/apthermeng

Research Paper

Analysis of an efficient liquified natural gas utilization cascade Brayton cycle and an improved cold energy recovery evaluation criterion

Gang Xiao [a,b], Yi Wu [a,b], Zheng Wang [a,b], Yafei Liu [a,b], Qinghe Guo [a,b], Zhangquan Wen [a,b], Dan Chen [a,b], Peiwang Zhu [a,b,*]

[a] Key Laboratory of Clean Energy and Carbon Neutrality of Zhejiang Province, Zhejiang University, Hangzhou, Zhejiang 310027, China
[b] State Key Laboratory of Clean Energy Utilization, Zhejiang University, 38 Zheda Road, Hangzhou 310027, China

ARTICLE INFO

Keywords:
LNG utilization
Brayton cycle
Sensitivity analysis
Exergy destruction
Cold energy recover

ABSTRACT

The cold energy utilization of liquified natural gas is a promising solution for electricity generation systems to raise power output. In order to enhance cold energy recovery performance, here we propose a cascade Brayton cycle, which can efficiently utilize the waste heat from gas turbine and the cold energy of liquefied natural gas. The temperature pinch in natural gas evaporator is successfully reduced by adopting helium as the working fluid. The optimal working condition is determined through parametric sensitivity analysis, and the exergy and economic performance is assessed and compared. The design case outperforming high energy efficiency (68.61 %), competitive exergy efficiency (58.51 %) and excellent levelized cost of electricity (0.0481$\$\cdot(\mathrm{kW\cdot h})^{-1}$). Moreover, the exergy destruction in natural gas evaporator reduced by 4.05 MW, resulting in 23.2 % improvement compared to conventional systems. Simultaneously, a modified criterion of "real specific work contributed per kg/s liquified natural gas" is proposed, which provides a more accurate cold energy recovery evaluation method for cold energy utilization power systems. The comparison of reported cold energy utilization systems are conducted based on the modified criterion, and our model delivers the best result among them.

1. Introduction

With the growing need to reduce air pollution and reach carbon neutrality, natural gas has attracted remarkable attention as an environmental-friendly energy source. It produces negligible amounts of nitrogen oxides, sulfides, and ash during combustion [1]. Moreover, the lower heating value of natural gas with compact storage is 47.5 MJ/kg [2], which is 1.6 times higher than that of standard coal in China. As a result, relevant institutions predict that natural gas with demand expected to rise by over 65 % from 2010 to 2040 [3]. Liquified natural gas (LNG), is produced through cryogenic refrigeration from gaseous state at low temperature of −162 °C [4]. Due to its high density, LNG can reduce storage volume by 600 times [5], making it more suitable for long-distance transportation and storage. LNG requires gasification before being utilized further, during the gasification process, nearly 830 kJ/kg of cold energy is released [6] to the atmosphere that is wasted. Therefore, the effective utilization of LNG cold energy is considered in recent years.

To date, the cold energy released during LNG gasification is commercially used in air separation [7,8], cold energy power generation [9], carbon dioxide capture [10,11], seawater desalination, food refrigeration, and potentially applied in data center cooling [12–15], energy storage [16] in the future. In terms of cold energy electricity generation, LNG works as heat sink to enhance the system operating efficiency. Rankine cycle is the common form of LNG cold energy power generation, in which the working fluid is heated by environmental heat and condensed by evaporating LNG. Direct expansion cycle is another way to recycle wasted cold energy by pre-pressurizing LNG to a higher pressure and expanded after heating. These technologies have been successfully employed in series LNG terminal [17–22]. However, the cold energy cannot be fully utilized and overall efficiency is limited under relatively low value [10].

In recent decades, numerous attempts have been made to further raise LNG cryogenic power system performance, which led to the development of complex systems [23–27]. Sun [28] studied different patterns of Rankine cycle integrated with LNG cold energy. He categorized them into three types: single-stage Rankine cycle, parallel-stages

* Corresponding author at: Key Laboratory of Clean Energy and Carbon Neutrality of Zhejiang Province, Zhejiang University, Hangzhou, Zhejiang 310027, China.
E-mail addresses: xiaogangtianmen@zju.edu.cn (G. Xiao), 22127052@zju.edu.cn (Y. Wu), 11927096@zju.edu.cn (Z. Wang), 12027088@zju.edu.cn (Y. Liu), qinghe@zju.edu.cn (Q. Guo), 12227078@zju.edu.cn (Z. Wen), 22227126@zju.edu.cn (D. Chen), zhupw@zju.edu.cn (P. Zhu).

https://doi.org/10.1016/j.applthermaleng.2024.123024
Received 14 October 2023; Received in revised form 7 January 2024; Accepted 20 March 2024
Available online 21 March 2024
1359-4311/

Nomenclature

Terminology

Ex	exergy (MW)
h	specific enthalpy ($MJ\cdot kg^{-1}$)
I	exergy loss (MW)
m	mass flow(kg/s)
P	pressure (MPa)
s	specific entropy ($MJ\cdot kg^{-1}\cdot K^{-1}$)
T	temperature (℃)
ΔT	temperature difference (℃)
$\Delta \overline{T}$	logarithmic mean temperature difference (K)
UA	total conductance of heat exchanger ($MW\cdot K^{-1}$)
V	volume (m^3)
W	power (MW)
η	efficiency
ξ	exergy factor
κ	adiabatic index

Abbreviations

CRF	Capital recovery factor
GWP	global warming potential
HX	heat exchanger
LCOE	Levelized cost of electricity $\$\cdot(kW\cdot h)^{-1}$
LHV	lower heating value
LNG	liquefied natural gas
NG	natural gas
ODP	ozone depletion potential
ORC	Organic Rankine cycle
RSPC	real specific power contributed per kg/s LNG
SPD	specific power developed per kg/s LNG
T	turbine

Subscripts

C	compressor
Chemistry	chemistry exergy
cold	cold exergy
cool	cooling process
dg	design case
F	fuel
g	generator
gt	gas turbine
i	number of different power cycle or components
in	inlet
is	isentropic process
net	net output
out	outlet
p	pump
pol	polytropic process
t	turbine
tot	total exergy input
Wf	working fluid
0	ambient condition

Superscripts

n	polytropic index
0	reference point

Rankine cycle and cascade-stage Rankine-cycle. The thermodynamic performance of these power cycles under various working fluid and working conditions are compared. The results indicated that the cascade-stage type can achieve higher exergy efficiency by dividing the working temperature range into different zones, this is particularly advantageous when deal with large temperature zones. On the other hand, when the temperature difference between the heat and cold sources is small, the parallel-stage type could achieve higher exergy efficiency. Wang [10] constructed a parallel-cascade combined Rankine cycle system for carbon capture using LNG as cold source and magnesite processing industry heat as heat source, which is operating under 100 °C so that the organic fluids can maintain thermostability. Simulation results highlighted that the majority of energy losses occurred at the heat exchanger, accounting for more than 90 % of the total system exergy losses. Therefore, it is crucial for system design to select appropriate working medium so that it can match LNG evaporation temperature and maintain a stable state. Liu [29] et al constructed a Rankine cycle with a mixed ethylene-propane composition and compared it with organic Rankine cycle using pure propane. The results demonstrated that the mixture enabled a better physical property, allowing for a reduced temperature difference during LNG evaporation process.

Brayton cycle is another common pattern that using non-condensable gas as working fluid. She [30] utilized N_2 as circulating fluid to recover cold energy of LNG and utilized waste heat of liquid air energy storage system, the result indicates that the N_2 Brayton cycle improves the exergy efficiency of the original standalone system up to 14.4 %. Ma [31] selected N_2 and CO_2 as working fluid and dual-stage Brayton cycles are modeled. The results show that cascade Brayton cycle configuration of LNG cold energy power generation system has better cold energy recovery performance while the parallel configuration has greater advantages in thermodynamic efficiency. The author also pointed out that the thermodynamic efficiency of the system depends largely on the design of the LNG evaporation heat exchanger. Gomez [32] also proposed a He/H_2O cascade Brayton-Rankine cycle, driven by high temperature steam of 1000 °C. This system achieved higher thermodynamic efficiency of 65.61 %, which is higher than most published combined system owing to helium can maintain good stability and heat conductivity at high temperature, but it causes relatively large exergy losses, due to the irreversible heat transfer process occurring inside the boiler. Cao [33] proposed a multi-cascade LNG cold energy power generation system combined with gas turbine unit where the exhaust gas from the combustion engine worked as the heat source. The system consists of a supercritical CO_2 Brayton cycle and a *trans*-critical CO_2 Rankine cycle, the results indicated that the utilization of cold energy with the waste heat of the exhaust gas can significantly improve the system thermodynamic performance, which provides an effective approach for utilizing the exhaust gas heat from gas turbine outlet. However, due to the triple phase point of CO_2 at −53 °C, over 80 °C of temperature pinch inside the heat exchanger between CO_2 and LNG, resulting in significant cold exergy destruction.

Many scholars have proposed coupling LNG cold energy with other systems, such as compression jet cooling [34], ocean thermal energy conversion (OTEC) [35], Allam cycle [36,37], and solid oxide fuel cell (SOFC) [38]. Kanbur [27,39] combined LNG cold energy with Stirling machine and developed a combined cycle using the waste heat from the gas turbine unit as the heat source for the Stirling machine, nitrogen was chosen as the working fluid in the Stirling machine. The authors analyzed the system thermodynamic performance, thermal-economic performance, and sustainability. The results demonstrated that the cascade Stirling cycle effectively improved the system performance in mentioned aspects, as well as 7.8 % increase of net power.

Due to the large temperature difference during LNG evaporation heat transfer process, amounts of irreversible losses occur at the heat exchanger that hinder further improvements in cold energy recovery performance. However, there is lack research addressing this issue. Therefore, this paper proposes a modified cycle combined with gas

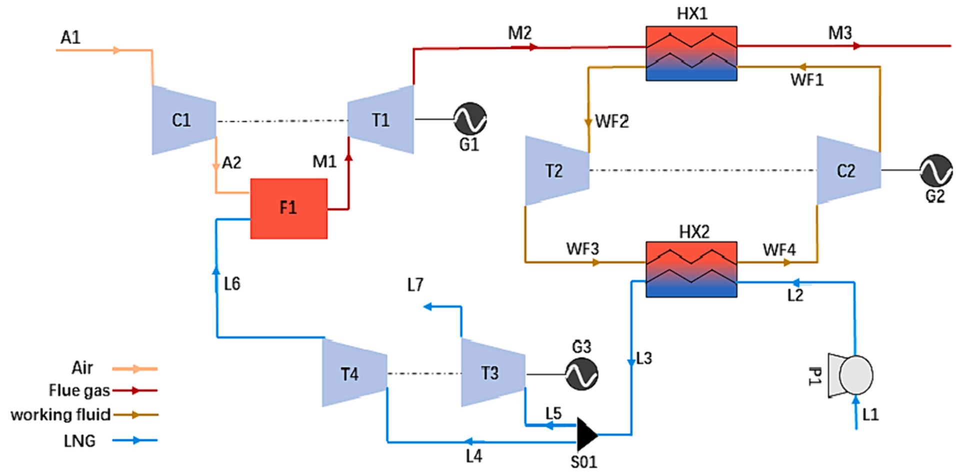

Fig. 1. Schematic diagram of modified cascade cycle.

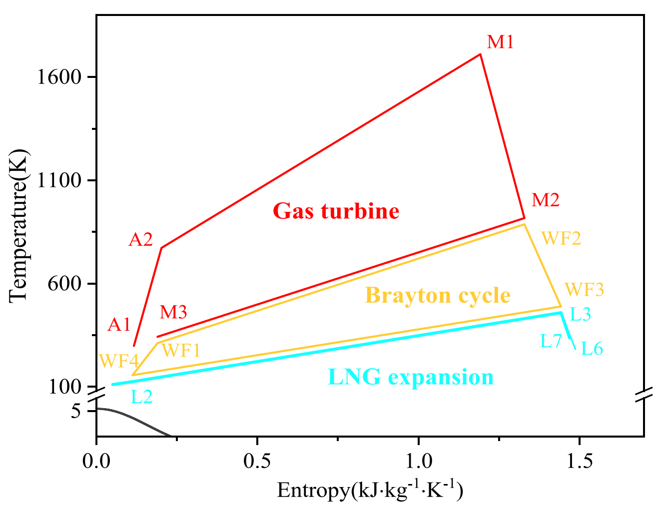

Fig. 2. T-S diagram of the proposed cascade Brayton cycle.

turbine and LNG cold energy utilization, adopting helium as the working fluid to reduce the irreversible heat transfer losses in heat exchangers via temperature pinch reduction. Sensitivity of temperature pinch is analyzed, exergy and economic performance evaluated and the superiority of the system is highlighted by comparing with conventional power systems. It is worth mentioning that we also proposed a modified evaluation criterion to assess the cold energy recovery performance, as the result, a more accurate result is demonstrated in LNG cold energy utilization systems.

2. System description and method

2.1. System configuration

The configuration of proposed system is illustrated in Fig. 1. The system is comprised of a gas turbine, a Brayton cycle and LNG direct expansion cycle. The exhaust gas is cooled by the LNG, which functions as both a heat sink and a fuel. A portion of the evaporated LNG is supplied to the combustion chamber after the energy has been released, while the remainder is transported through the pipeline at a specific temperature and pressure.

The design criterion of gas turbine unit is according to the GT36-S5 gas turbine, produced by Ansaldo Energia, with a power output up to 538 MW, and 621 °C of exhaust gas temperature, respectively [40]. The exhaust gas after expansion is cooled by Brayton cycle working fluid in

Table 1
Properties of the candidates used in Brayton cycle [47].

Pressures (MPa)	Helium	Nitrogen	Argon
Isobaric heat capacity(kJ/kg·k^{-1})			
0.1	5.19	1.07	0.52
2	5.19	1.10	0.54
4	5.19	1.13	0.57
Thermal conductivity(W/m·k^{-1})			
0.1	0.225	0.039	0.027
2	0.226	0.040	0.027
4	0.227	0.041	0.028

HX1, the multiple cascaded heat exchanger is not employed considering that the temperature of flow M3 is relatively low.

As for Brayton cycle, which can recover both cold energy from LNG and heat from exhaust gas, has an important impact on thermodynamic performance of integrated power cycle. The working fluid in the Brayton cycle is heated and cooled directly by the exhaust gas and LNG.

The LNG direct expansion cycle in the bottom of the integrated power cycle is processed as direct expansion. The evaporated LNG with thermal energy and pressure energy is expanded in T3 and T4, with varied back pressure due to the different application scenario of natural gas.

Fig. 2 illustrate the thermodynamic T-S diagram of the whole path. The working fluid of intermediate cycle is operating above saturation line hence the Brayton cycle is implemented. Better working performances is exhibited due to the temperature difference during heat transfer process is minimized, the superiority of the system is further verified on following discussions.

2.2. Cycle pattern and working fluid selection

In this work, the exhaust gas from gas turbine has a high temperature above 600 °C, which is destructive for most organic Rankine cycle working fluids [41] due to the lack of thermal stability at temperature above 400 °C [42–44]. The other Rankine cycle candidates H_2O and CO_2 [45] has a higher triple point temperature, with 0 °C and −53 °C, which means larger exergy loss would happen during cold transfer process. In contrast, using non-condensing fluid could exhibit low exergy loss by recovering cold energy in temperature around −160 °C, which is closer to LNG evaporating temperature. Cascaded Brayton/Rankine cycle is another alternative solution adopted in other researches. However, more heat exchangers are needed, and exergy efficiency would decrease as large proportion of exergy loss happened during heat transfer.

The first criterion of selecting working fluid is stability at high temperature (600 °C) and low temperature (−162 °C). Non-toxic, non-

Table 2
Previous assumption and working conditions.

Items	Gas turbine
Methane LHV (kJ/kg)	50,010[55]
NG distributed pressure (MPa)	6[56]
Air compressor polytropic efficiency (%)	0.915[57]
Turbine isentropic efficiency (MPa)	90[58]
Pump isentropic efficiency (%)	85[59]
Mechanical efficiency (%)	98[59]
Generator efficiency (%)	99[60]
Pressure dropped in heat exchanger (%)	2[61]
Environmental temperature (K)	293.15

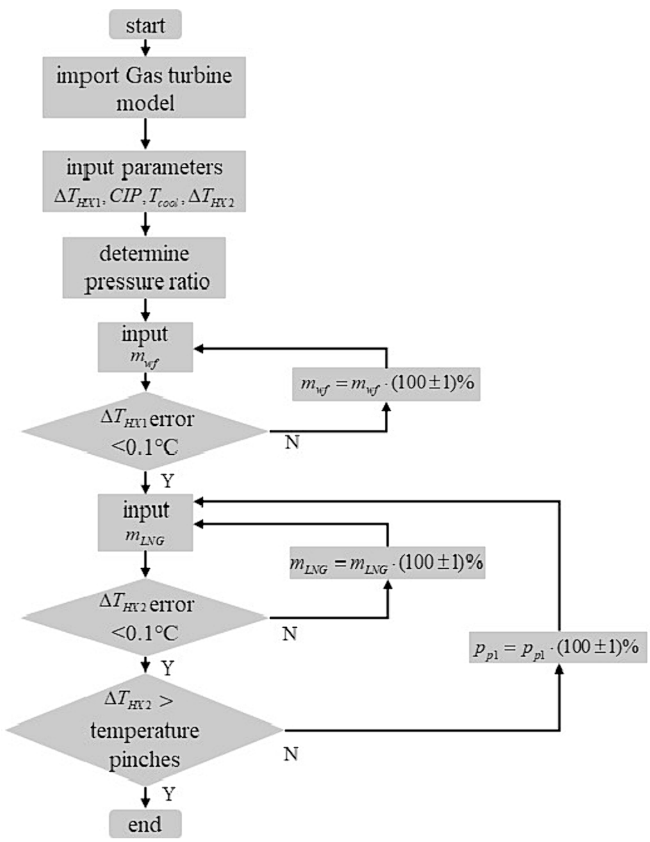

Fig. 3. Cases calculation procedure of system.

explosive, and non-flammable properties are subsequent demand for safety consideration. Low ODP and GWP values are desired but not compulsory. The candidates include helium, nitrogen and argon, all of them has low saturation temperature. Nevertheless, helium has more superior heat transfer characteristic, and is commonly used in nuclear power plant to cool the reactor for its good conductivity [46]. Table 1 presents the average isobaric heat capacity and thermal conductivity of the candidates from −100 °C to 600 °C, which is obtained from REFPROP database. As indicated in the table, the value of nitrogen and argon is approximately 4.7 and 9.6 times smaller than helium, which increasing the risk of uneven heat transfer and heat deterioration in heat transfer. Consequently, the working fluid selected in this paper is helium.

2.3. Method

The modelling process is carried out by ASPEN PLUS V10, a commercial software licensed by Aspen Tech. The thermodynamic properties of the working fluids are determined by mixing rules in software and Peng-Robinson equation [48], for its good ability predicting working fluids equation of state [49].

Several assumptions are made below to simplify the mathematical models and calculating process, and the further detailed assumption is listed in Table 2.

(1) The system operates at steady state [50].
(2) The inlet air is considered as a mixture of 21 mol% oxygen and 79 mol% nitrogen.
(3) LNG is considered as a pure methane [26,51].
(4) The pressure drop in pipeline of the system is ignored [10].

The optimization algorithm for this study is implemented on the MATLAB platform. The solving procedure follows the flow chart depicted in Fig. 3, which progresses according to the gas turbine - Brayton cycle - LNG expansion path. Four parameters are treated as variables in the algorithm, the pressure ratio and flowrate of the Brayton cycle are calculated iteratively based on given boundary conditions, and the LNG pumped pressure and flow rate are determined based on the heat exchanger conditions. Variable LNG pressure here is adjusted to eliminate the pinch point effect, resulting from LNG with different pressures has different phase change temperatures, heat capacity values, and enthalpy gained during the pumping process. Consequently, varying the LNG pumped pressure would result in different inlet thermal properties and finally impact the heat transfer profile. Fig. 4, as examples, present the temperature profile of both cold and hot streams in HX2, employing variable LNG pressure while hot side temperature remains constant, the result indicated that the pinch point effect is eliminated and the risk of heat transfer characteristic deterioration is mitigated.

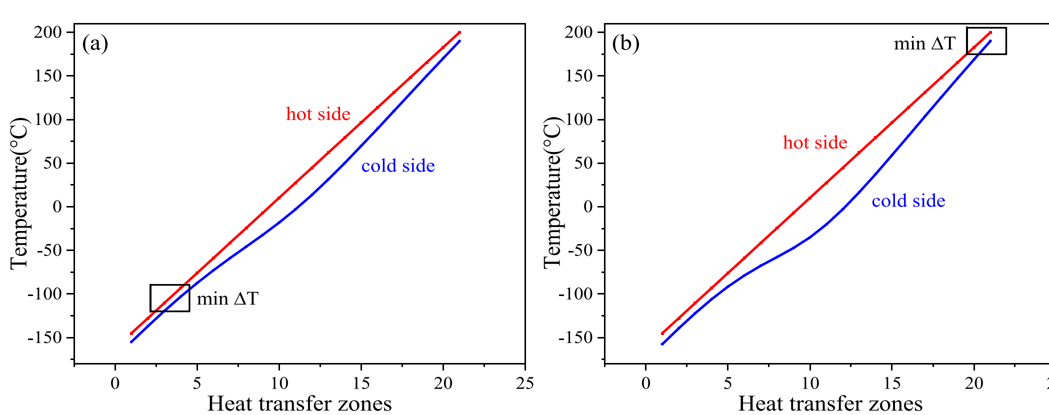

Fig. 4. Heat transfer profile of helium at 0.5 MPa, 200 °C and (a)LNG at 16 MPa (b) LNG at 10 MPa.

The algorithm employs a convergence criterion based on the design temperature difference and temperature pinches, with an absolute error tolerance of 0.1 °C. The algorithm records the operating performance under different working conditions, and eventually identifies the optimal working condition based on the recorded data.

3. Modelling

3.1. Gas turbine

The model of gas turbine is a combination of air compressor, combustion chamber and turbine, based on their thermodynamics principle and working condition, respectively.

In respect of air compressor unit, the polytropic process model is adopted. The polytropic process is expressed as [52]:

$$PV^{n} = \text{constant} \tag{1}$$

The exponent n is called the polytropic index and the value of it depends on the selected fluid and its physical parameters, the polytropic efficiency η_{pol} is defined by [53]:

$$\eta_{pol} = \frac{\kappa \ln(T_{out} - T_{in})}{(\kappa - 1)\ln(P_{out}/P_{in})} \tag{2}$$

The subscript *out* and *in* represent the parameters of air at the outlet and inlet of air compressor, respectively.

In respect of turbine, the isentropic efficiency is adopted to describe the energy conversion process at design condition, the isentropic efficiency is defined as [51]:

$$\eta_{is} = \frac{h_{in} - h_{out}}{h_{in} - h_{out,is}} \tag{3}$$

The energy efficiency of gas turbine can be expressed as [54]:

$$\eta_{gt} = \frac{W_t - W_c}{m_f \eta_g LHV_f} \tag{4}$$

3.2. Brayton cycle

The Brayton cycle consists of a compressor, turbine and two heat exchangers. The compressor and turbine are worked as a non-isentropic process, which is described by an isentropic efficiency η_{is}. The work produced and consumed by turbine and compressor are expressed as Eq. (5) and (6):

$$W_t = m_{wf} \eta_g (h_{WF2} - h_{WF3}) \tag{5}$$

$$W_c = m_{wf} (h_{WF1} - h_{WF4}) / \eta_g \tag{6}$$

The discretization method is adopted in each heat exchanger to calculate the heat transfer area, the properties of fluid in every subsection is assumed as constant and the fluid is assumed as counter flow. The total heat transfer is the sum of heat transfer happened in each subsection, which is defined as [23]:

$$Q = UA\Delta\overline{T} \tag{7}$$

Where Q is the heat transfer rate, U denotes the heat transfer coefficient, and $\Delta\overline{T}$ is the logarithmic mean temperature difference of hot and cold fluid in each subsection.

3.3. LNG direct expansion

The LNG direct expansion is worked as opened cycle, the work consumption is expressed as [30]:

$$W_P = m_{LNG} (h_{L2} - h_{L1}) / \eta_g \tag{8}$$

The evaporated natural gas with high pressure expanded through T3 and T4 in parallel, with an isentropic efficiency $\eta_{is,t}$, the former is expansion to a pressure of combustion chamber while the latter expansion to a distribution pressure. In this paper, the commonly scenarios, medium distance transportation, is considered. Consequently, the distribution pressure is determined as 6 MPa.

Table 3
Model validation of gas turbine.

Items	GT36-S5	This work	Error (%)
Power output (MW)	538	531	1.3
Energy efficiency (%)	42.8	42.0	0.8
Exhaust mass flow (kg/s)	1020	1028	0.8
Exhaust temperature (°C)	621	624	0.4

Table 4
Model validation of bottoming cycle.

Items	Ref[32,58]	This work	Error (%)
Brayton cycle			
Heating temperature (°C)	900	907.4	0.82
Pressure ratio	2.53	2.52	0.40
Temperature ratio	3.81	3.83	0.55
Turbine specific work (kJ/kg)	1699.8	1700.8	0.05
Net specific work (kJ/kg)	888.6	876.1	1.41
LNG expansion			
Pump outlet pressure (MPa)	27.54	27.95	1.50
Turbine outlet temperature (°C)	3.60	3.47	3.61
Turbine power output (kW)	158.24	154.37	2.45

3.4. Model validation

To guarantee the accuracy of the established system and calculation methods, the previous validation was proceeded based on divided parts. The calculated result of gas turbine is compared with claimed conditions of GT36-S5 [40], while the bottom cycle is conducted based on the models in other research data. The results showed acceptable accuracy as listed in Table 3 and Table 4.

4. Results and discussions

In this chapter, the effect of key parameters is investigated based on the optimal operating rules. The gas turbine unit is assumed to remain the design condition while the working condition of closed Brayton cycle and LNG expansion is adjustable according to the input parameters. Thermodynamic analysis is first conducted to acquire the operating characteristic of the system, and the optimal working condition is determined. The exergetic and economic performance are analyzed based on the result of optimal working condition, the superiority of the system is highlighted by comparing with conventional power cycles. Moreover, a modified evaluation criteria *RSPC* was introduced to this system, further comparison of *RSPC* between relevant systems is developed, and the factors contributed to the value of *RSPC* are evaluated.

4.1. Thermodynamic analysis

Fig. 5 illustrates the influence of T_{cool} and ΔT to the system energy efficiency. Higher pressure of LNG supply pump can typically recover more net power after LNG expansion, but higher cooling temperature is achieved with the increasing LNG pressure, which raise the helium compressor inlet temperature. Fig. 5(a) confirms this effect that with the T_{cool} increases from −149 °C to −135 °C, the overall energy efficiency grows rapidly at first and drops slightly after reaching its maximum.

In terms of temperature difference, increasing ΔT_{HX2} and ΔT_{HX1} have negative effect to the system efficiency. The variation of ΔT_{HX2} has more significant impact than ΔT_{HX1}, with 1 K of increased ΔT_{HX2} could lead to

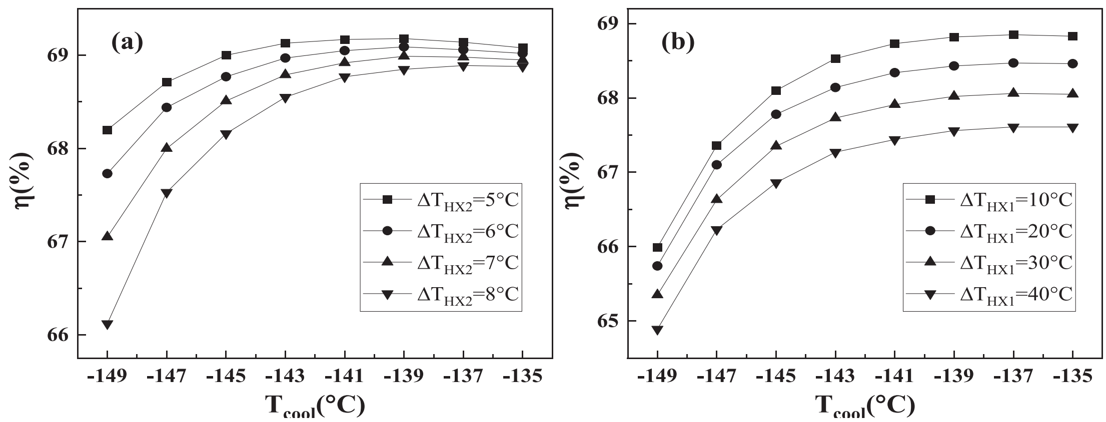

Fig. 5. Influence on efficiency according to (a)T_{cool},ΔT_{HX2}. (b) T_{cool},ΔT_{HX1}.

as high as nearly 1 % of efficiency drop. While approximately 1 % of efficiency decrease needs ΔT_{HX1} increases 20 K. Therefore, compared with high-temperature heat exchangers, the design and optimization of low-temperature heat exchangers require more comprehensive consideration.

4.2. Exergy analysis

Instead of water or air cooling, the power cycle in the current system is driven by both hot exergy from combusted flue gas and cold exergy of LNG. Hence the exergy efficiency is calculated as:

$$\eta_{ex} = \frac{W_{net}}{Ex_{cold} + Ex_{chmistry}} \tag{9}$$

In this equation, the denominator is divided by two parts, which is cold exergy contributed to the evaporation of LNG, and chemical exergy released by combusting natural gas, which are defined as below [62]:

$$Ex_{cold} = m_{L2}\cdot\left[h_{L2} - h^0_{L3} - T_0\left(s_{L2} - s^0_{L3}\right)\right] \tag{10}$$

$$Ex_{chemistry} = \xi\cdot m_{L6}\cdot LHV_f \tag{11}$$

Where ξ represents the exergy factor, which is taken by 1.04 [63,64] in this paper. Due to the natural gas is heated up from subcooled to superheated state in HX2, the superscript "0″ represents the reference point that the working fluids no longer has cold exergy, which is the point that temperature equal to ambient temperature. Exergy efficiency reflects the overall energy utilization but cannot identify the exergy loss in each component. Hence, the components exergy destruction is calculated below, to further evaluate system exergy performance.

The exergy gained or dropped in heat exchangers is defined as the exergy difference at the inlet and outside of specified side, the exergy loss happened in heat exchangers is due to the irreversibility during heat transfer process [25]. As an example, the cold exergy gained of working fluid and exergy loss in HX2 is calculated as Eq. (12) and Eq. (13), respectively.

$$Ex_{HX2,wf} = m_{WF3}\cdot\left[h_{WF4} - h_{WF3} - T_0\left(s_{WF4} - s_{WF3}\right)\right] \tag{12}$$

where exergy loss is defined as:

$$I_{HX2} = Ex_{cold} - Ex_{HX2,WF} \tag{13}$$

The exergy loss in pump/compressor is mainly caused by friction loss, which is defined as the difference of work consumed and exergy gained, the process happened in C2 is:

$$Ex_{C2,wf} = \left[h_{WF1} - h_{WF4} - T_0\left(s_{WF1} - s_{WF4}\right)\right] \tag{14}$$

$$I_{C2} = W_{C2} - Ex_{C2,WF} \tag{15}$$

While on the other hand, the exergy loss in expander is calculated as the difference of the exergy decrease of working fluid and the work produced, in T2 is:

Fig. 6 Illustrates how the system exergy performance varies with the parameters. As temperature difference of hx2 increases, there is a sharp rise in exergy loss during heat transfer. The influence of varied LNG pressure is depicted in fig.6(b), as the pressure increases, more expansion power could be recycled and the exergy efficiency increases. However, when the pressure exceeds 28 MPa, the pinch point effect happened as the minimum temperature difference is lower than 10 K. Further increasing the pressure of LNG leads to more obvious pinch

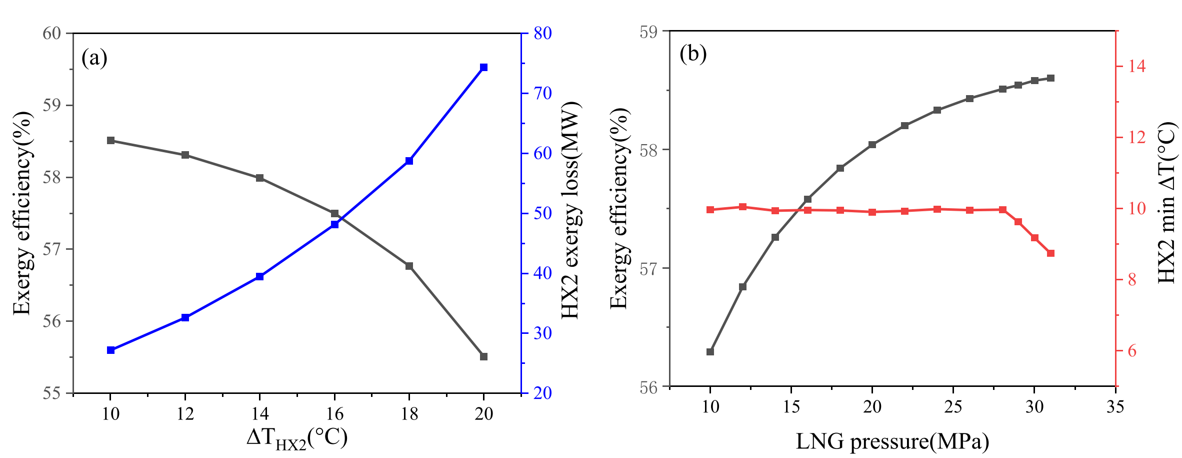

Fig. 6. HX2 working performances varied with (a) ΔT_{HX2} and (b) LNG pressure.

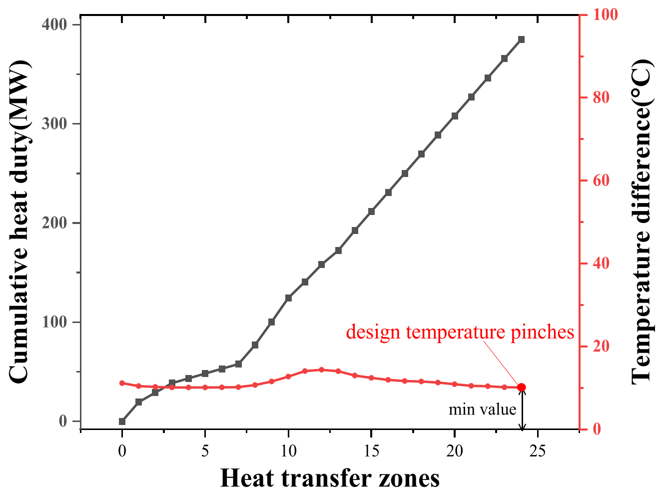

Fig. 7. Cumulative heat duty-temperature difference line in HX2.

Table 5
The economic index assumptions.

Items	Value
Discount rate (%)	6[66]
Operation lifetime (year)	20[66]
Auxiliary system cost rate (%)	7.5[65]
Fuel cost ($/GJ)	8.588[67]
Annual maintenance cost rate (%)	0.015[65]
Annual labor cost ($)	20*40000[65]
Annual insurance cost rate (%)	0.01[65]
Annual operation hour (h)	7000[67]

point effects while system exergy efficiency has a limited increase. Therefore, the pressure at this turning point was chosen as design pressure.

The results of exergy balance are shown in Appendix Table A.1. The exergy loss in LNG evaporator, which is considered as the mainly exergy destruction in past studies, accounting for 1.85 % of the exergy destruction in this work, keep at the same level with exhaust gas heat exchanger. The main reason is the temperature difference of working fluid and LNG at inlet of HX2 can be kept at a low value. Fig. 7 shows the temperature difference-heat relationship in HX2, the result confirm that the total exergy destruction could be significantly reduced by minishing working fluid heat transfer temperature difference.

4.3. Economy analysis

In this section, the economic index LCOE (levelized cost of electricity, $\$\cdot(\mathrm{kW}\cdot\mathrm{h})^{-1}$) is used to further evaluating the cost-effective characteristic of the proposed system. The equation can be expressed below [65]:

$$LCOE = \frac{CRF \cdot C_{TPC} + C_{O\&M}}{W_{net}} \tag{18}$$

where CRF represents the capital recovery factor, C_{TPC} is the total investment of the whole system while $C_{O\&M}$ denotes the operation and maintenance cost. The equation is calculated as [65]:

$$CRF = \frac{i \cdot (1+i)^N}{(1+i)^N - 1} \tag{19}$$

$$C_{TPC} = \sum C_c + C_{aux} \tag{20}$$

$$C_{O\&M} = C_{fuel} + C_{maint} + C_{lab} + C_{ins} + C_e \tag{21}$$

Table 6
Performance comparison with conventional power cycles.

Items	This work	gas-steam combined cycle	gas-steam combined cycle + ORC
LNG supply flow (kg/s)	341.26	–	341.26
Fuel consumed (kg/s)	25.30	25.30	25.30
Total power output (MW)	868.30	786.51	797.50
Energy efficiency (%)	68.61	62.67	63.55
Exergy efficiency (%)	58.51	59.74	54.20
Exergy loss in LNG evaporator (MW)	27.16	–	120.61
Exergy loss in exhaust gas heater (MW)	13.41	17.46	17.46
LCOE ($\$\cdot(\mathrm{kW}\cdot\mathrm{h})^{-1}$)	0.0481	0.0530	0.0525

where i is the discount rate and N is the operation lifetime of the system. The C_{TPC} consists of investment of each component and auxiliary system of the components cost. $C_{O\&M}$ includes the cost of fuel, maintenance, labor, insurance and plant electricity, the value assumed for the index is shown in Table 5.

Each component investment is calculated from the equations [65,67–71] in Supplementary files Table B.1, according to their working parameters and performances. The evaluation method is also performed on other conventional power cycles, to further evaluate the superiority of the proposed system.

4.4. Case results

Herein, the design case is determined according to the conducted analyses, the working parameters of each stream flow is shown in Appendix Table A.2. The exhaust heat of selected gas turbine could match 341kg/s LNG while 25kg/s of them is combusted. The system thermodynamic efficiency and exergy efficiency are 68.61% and 58.51%, respectively. The total power output is 868.30MW, of which G1, G2, G3 contribute 531.2MW, 275.1MW and 62.0MW, respectively. The essential performance of the design case is compared with two conventional power cycles in LNG terminal, which is gas-steam combined cycle, and gas-steam combined cycle with a standalone organic Rankine cycle, using propane as working fluid. The result as shown in Table 6, the prototype of gas turbine is consistent with this paper and the data is validated with the published paper and reports [40,72]. The energy efficiency increases 5.94% and 5.06% when compared with two conventional systems, although gas-steam combined cycle exhibited higher exergy efficiency, the large amount of exergy loss during LNG evaporation in organic Rankine cycle impedes the further enhancement of system. It is worth mentioning that the exergy destruction in LNG evaporator reduced by 4.05 MW, corresponding to a 23.05% improvement. The economic analysis also shows advantage in terms of LCOE, which decreases 9.25% and 8.38% cost when compared with other two power systems.

4.5. RSPC

To further acquire cold energy utilization system power generation characteristic, an indicator of "specific power developed per kg/s of LNG" (SPD) is reported, which is calculated by total net power produced per mass flow of LNG [62], as defined in Eq. (22).

$$SPD = \frac{W_{net}}{m_{LNG}} \eta_g \tag{22}$$

This indicator could get accurate result in common scenario. However, it may be inaccurate in the case where the net power produced in a system not only converted from cold energy of LNG, but also from heat sources. For instance, the calculation result of SPD is accurate in a case that a power system utilizing sea water to recover LNG cold energy,

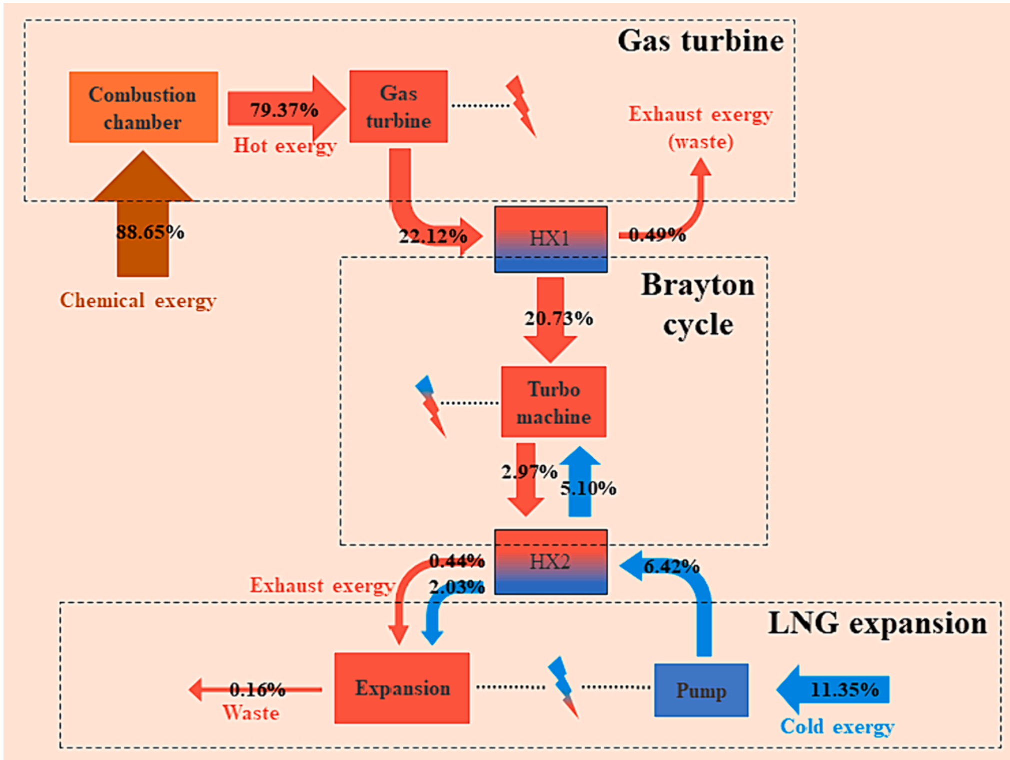

Fig. 8. The hot and exergy flow in the proposed system.

considering that there is no extra exergy input except cold exergy. However, the result is invalid when other heat source like exhaust heat is introduced to the system, due to a part of work produced is contributed to hot exergy. Consequently, it is necessary to introduce an exergy analysis method to accurately identify the power that is contributed to the cold exergy. Hence, the indicator real specific power contributed per kg/s LNG (*RSPC*) is proposed and the definition is:

$$RSPC = \left(\sum_{i=1}^{i=n} \frac{Ex_{cold}(m)}{Ex_{tot}(m)} W_{net,i}\eta_g\right)/m_{LNG} \tag{23}$$

The subscript *i* denotes the number of different power cycle which can convert cold exergy to work, *tot* denotes the total exergy input to the power cycle while the subscript *cold* means the exergy input to the power cycle contributed by the cold energy of LNG. In this way, the real power output contributed by cold energy is modified by the cold exergy ratio.

To further demonstrate RSPC, the proposed system, as an example, the hot and cold exergy flow is illustrated in Fig. 8. The system exergy input of design case is divided by chemical exergy (88.65%) and cold exergy (11.35%), the hot and cold exergy flow in each component is calculated separately. According to the exergy flow diagram, a portion of power output from Brayton cycle and LNG expansion path are contributed to cold exergy, while the gas turbine unit was completely driven by hot exergy. Therefore, the specific power developed by LNG could be modified by calculating the proportion of hot and cold exergy involved. In the design case, *RSPC* is calculated by Eq. (24) and the result is 325.7 kJ/kg, much smaller than the value calculated with Eq. (22) under *SPD* rule, which is 2544.39 kJ/kg.

$$RSPC_{dg} = \frac{\left(\frac{Ex_{HX2,cold}}{Ex_{HX1,hot}+Ex_{HX2,cold}}(W_{T2}-W_{C2}) + \frac{Ex_{in,cold}}{Ex_{HX2,hot}+Ex_{in,cold}}(W_{T3}+W_{T4}-W_{p1})\right)\eta_g}{m_{L1}} \tag{24}$$

Where:

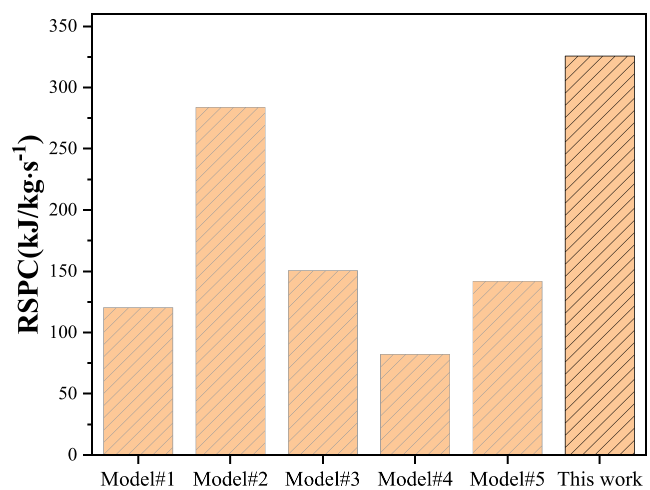

Fig. 9. Calculation results of models in Ref. [33,51,62,73,74].

$$\begin{aligned} & Ex_{HX2,cold} = Ex_{WF4} - Ex^0_{WF3} \\ & = m_{WF3}\cdot\left(h_{WF4} - h^0_{WF3} - T_0\left(s_{WF4} - s^0_{WF3}\right)\right) \end{aligned} \tag{25}$$

$$\begin{aligned} & Ex_{HX1,hot} = Ex_{WF2} - Ex_{WF1} \\ & = m_{WF1}\cdot\left(h_{WF2} - h_{WF1} - T_0\left(s_{WF2} - s_{WF1}\right)\right) \end{aligned} \tag{26}$$

$$\begin{aligned} & Ex_{HX2,hot} = Ex_{L3} - Ex^0_{L2} \\ & = m_{L2}\cdot\left(h_{L3} - h^0_{L3} - T_0\left(s_{L3} - s^0_{L2}\right)\right) \end{aligned} \tag{27}$$

The reference point is also adopted when evaluate hot and cold exergy gained for natural gas and helium, owing to the non-monotonic exergy changes between the states of subcooled and superheated.

To demonstrate the factor contributed to the value of *RSPC*, relevant model proposed by other researchers is also calculated here. In order to

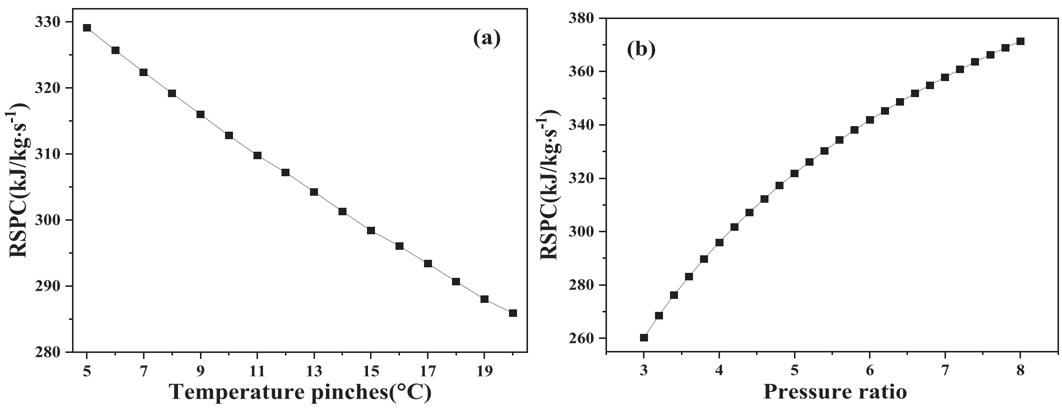

Fig. 10. Influence on *RSPC* according to (a)temperature pinches (b)distributed NG pressure.

conduct more comprehensive conclusions, the models selected have covered nearly all the available LNG cold energy utilization patterns. The respective model validation information is listed in Supplementary files Table B.1. and calculated result is illustrated in Fig. 9.

As illustrated in Fig. 9, the *RSPC* of models is plotted as bars graph. All the models shown here are operated as combined cycle that convert both cold exergy and hot exergy, the heat source include flue gas, exhaust gas and geothermal energy. Therefore, the proposed criterion could provide the result in a more accurate way, the modified value decreased by 22.19 %, 82.80 %, 86.23 %, 29.67 %, 89.46 % than previous value, respectively.

There are few factors contributed to the value of *RSPC*, one of the most essential factors is the temperature pinches in LNG evaporator, as mentioned previously. Larger temperature pinches causes more exergy destruction. Fig. 10(a) depicts the *RSPC* of the system with the varying temperature pinches at HX2, *RSPC* shows a significant reduction with an increase of heat transfer temperature pinches. It is supported by model#2, which exhibits higher result among others. model#2 adopts helium as a working fluid and kept outlet temperature of helium at LNG evaporator close LNG evaporating temperature. Although the model developed by model#4 used argon with a cooling temperature of −136.1 °C, the cycle flowrate is the relatively low. model#1 and model#5 both adopt CO_2 as a working fluid, resulting in a certain amount of exergy destruction happened inside the LNG evaporator.

The heating temperature also plays a significant role, higher heating temperature enables higher *RSPC* than other power cycle heated by environment, larger proportion of cold exergy could convert to work with higher temperature ratio. As shown in Fig. 9, model#4 adopts parallel method with argon and carbon dioxide to utilize the cold energy of LNG. However, the heating temperature of power cycle RC-2 and RC-3 is 51.47 °C and 7 °C, which is lower than other researches above.

Another important factor contributed to *RSPC* is the direct expansion path of LNG, which is adopted in this work and models of model#1 and model#2, the direct expansion path pumps the LNG to a higher pressure firstly and expands to distribute pressure after evaporating and heating. In LNG expansion path, the cold exergy can convert to expansion work directly that enables a more productively cold energy recovery. The value of *RSPC* is positively related to the expansion ratio, as depicted in Fig. 10(b), with the increases of pressure ratio of expansion path, the value of *RSPC* increases sharply. In published systems, the model developed by model#2 has an expansion ratio of 3.38, while model#1 also adopts LNG direct expansion path, the results did not show an obviously advantages due to the pressure ratio is relatively low at 1.58 and the heating temperature is also much lower than model#2, model#3, and model#5.

5. Conclusion

In this paper, a modified cascade Brayton cycle is proposed, which could fully utilize liquified natural gas cold energy for cold energy integration power system. The comprehensive analyses based on energy, exergy and economic performance is developed. Meanwhile, a modified criterion to evaluate cold energy recovery is investigated. The main conclusions are summarized as followed:

(1) The temperature difference during heat transfer process in the natural gas evaporator is essential for system efficiency and cold energy recovery performance. Helium is a suitable working fluid that could match both high temperatures over 600 °C and the low temperature of −162 °C.
(2) A parameters optimizing strategy is conducted and the design case achieves 68.61 % of energy efficiency, 58.51 % of exergy efficiency, 0.0481 $\$\cdot(\text{kW}\cdot\text{h})^{-1}$ of levelized cost of electricity, and the exergy destruction in natural gas evaporator reduced by 4.05 MW. The improvements reach as much as 5.94 %, 4.31 %, 8.38 % and 23.20 % when comparing with conventional power systems.
(3) A new criterion "real specific work contributed per kg/s liquified natural gas" is proposed to evaluate the cold energy recovery cold energy utilization system. This criterion develops a more accurate result by excluding the influence of hot exergy. Relevant models are developed to re-evaluate the results. In design case, the result is 325.7 kJ/kg, which is the highest among reported systems.
(4) Factors contributed to this criterion are analyzed, the results are supported by relevant models. The value of criterion can be effectively increased by reducing the temperature pinches in the LNG evaporator, increasing the expansion ratio of the LNG expansion path, and elevating the heat source temperature.

CRediT authorship contribution statement

Gang Xiao: Supervision, Writing – review & editing, Methodology, Resources. **Yi Wu:** Conceptualization, Data curation, Investigation, Methodology, Software, Validation, Writing – original draft. **Zheng Wang:** Conceptualization, Investigation, Methodology. **Yafei Liu:** Data curation, Investigation. **Qinghe Guo:** Data curation, Investigation. **Zhangquan Wen:** Data curation, Investigation. **Dan Chen:** Data curation, Investigation. **Peiwang Zhu:** Methodology, Resources, Supervision, Writing – review & editing.

Declaration of competing interest

The authors declare that they have no known competing financial interests or personal relationships that could have appeared to influence the work reported in this paper.

Data availability

Data will be made available on request.

Acknowledgement

The authors gratefully acknowledge the support from the National Natural Science Foundation of China (No. 52325605), the Key R&D Program of Zhejiang (No. 2022C01043) and the Fundamental Research Funds for the Central Universities (2022ZFJH04).

Appendix A

Table A1. The results of exergy loss in each component.

Symbols	I_i(MW)	Proportion (%)
I_{C1}	35.58	2.42
I_{F1}	373.96	25.45
I_{T1}	62.64	4.26
I_{HX1}	13.41	0.91
I_{C2}	28.22	1.92
I_{T2}	36.11	2.46
I_{HX2}	27.16	1.85
I_{P1}	21.34	1.45
I_{T3}	9.89	0.67
I_{T4}	1.29	0.09
Total loss	609.60	41.49
Total input	1469.28	100

Table A.2. Result of state points in design case.

State point	$m/(kg{\cdot}s^{-1})$	$T/(^\circ C)$	$p/(Mpa)$	$h/(kJ{\cdot}kg^{-1})$
A1	1002.84	15.00	0.101	−10.408
A2	1002.84	499.43	2.6	497.653
M1	1028.14	1438.11	2.55	368.630
M2	1028.14	624.00	0.103	−674.121
M3	1028.14	48.84	0.101	−1320.390
WF1	222.55	38.67	6.53	92.281
WF2	222.55	614.00	6.40	3077.943
WF3	222.55	196.04	1.00	891.468
WF4	222.55	−137	0.98	−838.512
L1	341.26	−162.00	0.101	−5555.830
L2	341.26	−148.10	28.05	−5473.225
L3	341.26	185.94	27.49	−4345.046
L4	25.30	185.94	27.49	−4345.046
L5	315.96	185.94	27.49	−4345.046
L6	25.30	9.40	2.65	−4712.560
L7	315.96	64.14	6.00	−4609.80

Appendix B. Supplementary data

Supplementary data to this article can be found online at https://doi.org/10.1016/j.applthermaleng.2024.123024.

References

[1] B.B. Kanbur, L. Xiang, S. Dubey, F.H. Choo, F. Duan, Cold utilization systems of LNG: a review, Renew. Sustain. Energy Rev. 79 (2017) 1171–1188.

[2] M.I. Khan, T. Yasmin, A. Shakoor, Technical overview of compressed natural gas (CNG) as a transportation fuel, Renew. Sustain. Energy Rev. 51 (2015) 785–797.

[3] R. Selin, The Outlook for Energy: a View to 2040 (2013).

[4] V.L. Bondarenko, O.V. Diachenko, T.V. Diachenko, Analysis of industrial LNG production technologies, Chem. Pet. Eng. 57 (2022) 985–996.

[5] I. Lee, K. Tak, H. Kwon, J. Kim, D. Ko, I. Moon, Design and optimization of a pure refrigerant cycle for natural gas Liquefaction with subcooling, Ind. Eng. Chem. Res. 53 (2014) 10397–10403.

[6] Y.Y. Li, Y.J. Liu, G.Q. Zhang, Y.P. Yang, Thermodynamic analysis of a novel combined cooling and power system utilizing liquefied natural gas (LNG) cryogenic energy and low-temperature waste heat, Energy 199 (2020) 117479.

[7] M.H. Hamayun, N. Ramzan, M. Hussain, M. Faheem, Conventional and advanced exergy analyses of an integrated LNG regasification-air Separation process, Ind. Eng. Chem. Res. 61 (2022) 2843–2853.

[8] Y.Q. Wu, Y.L. Xiang, L. Cai, H.T. Liu, Y. Liang, Optimization of a novel cryogenic air separation process based on cold energy recovery of LNG with exergoeconomic analysis, J. Clean. Prod. 275 (2020).

[9] T. He, Z.R. Chong, J. Zheng, Y. Ju, P. Linga, LNG cold energy utilization: prospects and challenges, Energy 170 (2019) 557–568.

[10] X. Wang, L. Zhao, L. Zhang, M. Zhang, H. Dong, A novel combined system for LNG cold energy utilization to capture carbon dioxide in the flue gas from the magnesite processing industry, Energy 187 (2019) 115963.

[11] M. Feenstra, J. Monteiro, J.T. van den Akker, M.R.M. Abu-Zahra, E. Gilling, E. Goetheer, Ship-based carbon capture onboard of diesel or LNG-fuelled ships, Int. J. Greenhouse Gas Control 85 (2019) 1–10.

[12] V. La Rocca, Cold recovery during regasification of LNG part two: applications in an agro food industry and a Hypermarket, Energy 36 (2011) 4897–4908.

[13] F.E. Ahmed, R. Hashaikeh, N.J.D. Hilal, Hybrid technologies: the future of energy efficient desalination–a review, Desalination 495 (2020) 114659.

[14] M.H. Noor Akashah, N.E. Mohammad Rozali, S. Mahadzir, P.Y.J.P. Liew, Utilization of cold energy from LNG regasification process, A Review of Current Trends, Processes 11 (2023) 517.

[15] Z.R. Chong, T. He, P. Babu, J.-N. Zheng, P. Linga, Economic evaluation of energy efficient hydrate based desalination utilizing cold energy from liquefied natural gas (LNG), Desalination 463 (2019) 69–80.

[16] E. Oró, A. de Gracia, A. Castell, M.M. Farid, L.F. Cabeza, Review on phase change materials (PCMs) for cold thermal energy storage applications, Appl. Energy 99 (2012) 513–533.
[17] A. Prabowo, S. Kartohardjono, Study of cryogenic power generation application at LNG regasification terminal, 3rd International Tropical Renewable Energy Conference Sustainable Development of Tropical Renewable Energy (I-Trec 2018), 67 (2018).
[18] N. Karashima, T. Akutsu, Development of LNG cryogenic power generation plant, in: In: Proc of 17th conference IECEC;, Vol. 1, 1982, pp. 399-404.
[19] H. Dhameliya, P. Agrawal, LNG cryogenic energy utilization, Energy Procedia 90 (2016) 660–665.
[20] Y. Hisazumi, Y. Yamasaki, S. Sugiyama, Proposal for a high efficiency LNG power-generation system utilizing waste heat from the combined cycle, Appl. Energy 60 (1998) 169–182.
[21] W. Lin, N. Zhang, A. Gu, LNG (liquefied natural gas): a necessary part in China's future energy infrastructure, Energy 35 (2010) 4383–4391.
[22] T. Mohri, K. Kawaguchi, K. Ichihara, O. Kita, A POWER GENERATING PLANT BY LNG COLD ENERGY, in: Yasukochi, Nagano (eds.) Proceedings of the Ninth International Cryogenic Engineering Conference, Kobe, Japan, 11–14 May 1982, Butterworth-Heinemann, 1982, pp. 705-708.
[23] W. Xia, Y. Huo, Y. Song, J. Han, Y. Dai, Off-design analysis of a CO2 rankine cycle for the recovery of LNG cold energy with ambient air as heat source, Energ. Conver. Manage. 183 (2019) 116–125.
[24] T. He, H. Lv, Z. Shao, J. Zhang, X. Xing, H. Ma, Cascade utilization of LNG cold energy by integrating cryogenic energy storage, organic rankine cycle and direct cooling, Appl. Energy 277 (2020) 115570.
[25] L. Zhao, J.L. Zhang, X. Wang, J.S. Feng, H. Dong, X.W. Kong, Dynamic exergy analysis of a novel LNG cold energy utilization system combined with cold, heat and power, Energy 212 (2020).
[26] Z. Sun, Z. Wu, Q. Zhao, X. Liu, K. Lin, Thermodynamic improvements of LNG cold exergy power generation system by using supercritical ORC with unconventional condenser, Energ. Conver. Manage. 223 (2020) 113263.
[27] B.B. Kanbur, L. Xiang, S. Dubey, F.H. Choo, F. Duan, Finite sum based thermoeconomic and sustainable analyses of the small scale LNG cold utilized power generation systems, Appl. Energy 220 (2018) 944–961.
[28] Z.X. Sun, F.Q. Xu, S.J. Wang, J.P. Lai, K. Lin, Comparative study of rankine cycle configurations utilizing LNG cold energy under different NG distribution pressures, Energy 139 (2017) 380–393.
[29] Y.N. Liu, Y.F. Ding, H. Wang, Y.H. Wang, Thermodynamics Analysis of a Novel Cryogenic Power Cycle for LNG Cold Energy Recovery with Binary Mixture as Working Fluid Vol. 205 (2017) 1946–1951.
[30] X. She, T. Zhang, L. Cong, X. Peng, C. Li, Y. Luo, Y. Ding, Flexible integration of liquid air energy storage with liquefied natural gas regasification for power generation enhancement, Appl. Energy 251 (2019).
[31] J. Ma, X.D. Song, B. Zhang, N. Mao, T.B. He, Optimal design of dual-stage combined cycles to recover LNG cold energy and low-temperature waste thermal energy for sustainable power generation, Energ. Conver. Manage. 269 (2022) 116141.
[32] M.R. Gómez, R.F. Garcia, J.R. Gómez, J.C. Carril, Thermodynamic analysis of a Brayton cycle and rankine cycle arranged in series exploiting the cold exergy of LNG (liquefied natural gas), Energy 66 (2014) 927–937.
[33] Y. Cao, J. Ren, Y. Sang, Y. Dai, Thermodynamic analysis and optimization of a gas turbine and cascade CO2 combined cycle, Energ. Conver. Manage. 144 (2017) 193–204.
[34] D.A. Dokandari, R.H. Khoshkhoo, M. Bidi, M. Mafi, Thermodynamic investigation and optimization of two novel combined power-refrigeration cycles using cryogenic LNG energy, Int. J. Refrig 124 (2021) 167–183.
[35] N. Arcuri, R. Bruno, P. Bevilacqua, LNG as cold heat source in OTEC systems, Ocean Eng. 104 (2015) 349–358.
[36] Z.L. Zhu, Y.P. Chen, J.F. Wu, S.B. Zhang, S.X. Zheng, A modified allam cycle without compressors realizing efficient power generation with peak load shifting and CO2 capture, Energy 174 (2019) 478–487.
[37] Y. Haseli, N.S. Sifat, Performance modeling of allam cycle integrated with a cryogenic air separation process, Comput. Chem. Eng. 148 (2021).
[38] K. Atsonios, C. Samlis, K. Manou, A. Nikolopoulos, K. Sfetsioris, A. Mitsotakis, P. Grammelis, Technical assessment of LNG based polygeneration systems for non-interconnected island cases using SOFC, Int. J. Hydrogen Energy 46 (2021) 4827–4843.
[39] B.B. Kanbur, L. Xiang, S. Dubey, F.H. Choo, F. Duan, Thermoeconomic and environmental assessments of a combined cycle for the small scale LNG cold utilization, Appl. Energy 204 (2017) 1148–1162.
[40] L.A. Bulysova, A.L. Berne, V.D. Vasil'ev, M.N. Gutnik, M.M. Gutnik, Study of sequential two-stage combustion in a low-emission gas turbine combustion chamber, Therm. Eng. 65 (2018) 806–817.
[41] S. Lecompte, H. Huisseune, M. van den Broek, B. Vanslambrouck, M. De Paepe, Review of organic rankine cycle (ORC) architectures for waste heat recovery, Renew. Sustain. Energy Rev. 47 (2015) 448–461.
[42] L. Calderazzi, P.C. di Paliano, Thermal stability of R-134a, R-141b, R-13I1, R-7146, R-125 associated with stainless steel as a containing material, Int. J. Refrig 20 (1997) 381–389.
[43] X. Dai, L. Shi, Q. An, W. Qian, Chemical kinetics method for evaluating the thermal stability of organic rankine cycle working fluids, Appl. Therm. Eng. 100 (2016) 708–713.
[44] D.M. Ginosar, L.M. Petkovic, D.P. Guillen, Thermal stability of cyclopentane as an organic rankine cycle working fluid, Energy Fuel 25 (2011) 4138–4144.
[45] F. Crespi, G. Gavagnin, D. Sánchez, G.S. Martínez, Supercritical carbon dioxide cycles for power generation: a review, Appl. Energy 195 (2017) 152–183.
[46] P. Norajitra, L.V. Boccaccini, E. Diegele, V. Filatov, A. Gervash, R. Giniyatulin, S. Gordeev, V. Heinzel, G. Janeschitz, J. Konys, W. Krauss, R. Kruessmann, S. Malang, I. Mazul, A. Moeslang, C. Petersen, G. Reimann, M. Rieth, G. Rizzi, M. Rumyantsev, R. Ruprecht, V. Slobodtchouk, Development of a helium-cooled divertor concept: design-related requirements on materials and fabrication technology, J. Nucl. Mater. 329–333 (2004) 1594–1598.
[47] E.W. Lemmon, I.H. Bell, M. Huber, M. McLinden, NIST standard reference database 23: reference fluid thermodynamic and transport properties-REFPROP, Version 10.0., in: National Institute of Standards and Technology, Standard Reference Data Program. , 2018.
[48] G. Zhang, J. Zheng, Y. Yang, W. Liu, A novel LNG cryogenic energy utilization method for inlet air cooling to improve the performance of combined cycle, Appl. Energy 179 (2016) 638–649.
[49] J. Xue, X. Nie, Z. Du, H.-R. Li, L. Zhao, Y. Zhu, J. Wang, Molecular dynamics investigation on isobaric heat capacity of working fluid in supercritical CO2 Brayton cycle: effect of trace gas, J. CO2 Util. 55 (2022).
[50] H.W. Choi, S.I. Na, S. Bin Hong, Y. Chung, D.K. Kim, M.S. Kim, Optimal design of organic rankine cycle recovering LNG cold energy with finite heat exchanger size, Energy 217 (2021).
[51] S.-H. Cha, S.-I. Na, Y.H. Lee, M.S. Kim, Thermodynamic analysis of a gas turbine inlet air cooling and recovering system in gas turbine and CO2 combined cycle using cold energy from LNG terminal, Energ. Conver. Manage. 230 (2021).
[52] R.A. Huntington, Evaluation of polytropic calculation methods for turbomachinery performance, J. Eng. Gas Turbines Power 107 (1985) 872–876.
[53] I.-H. Choi, S. Lee, Y. Seo, D. Chang, Analysis and optimization of cascade rankine cycle for liquefied natural gas cold energy recovery, Energy 61 (2013) 179–195.
[54] T. Lu, W. k.s.,, Analysis and optimization of a cascading power cycle with liquefied natural gas (LNG) cold energy recovery, Appl. Therm. Eng. 29 (2009) 1478–1484.
[55] N. Zhang, N. Lior, A novel near-zero CO2 emission thermal cycle with LNG cryogenic exergy utilization, Energy 31 (2006) 1666–1679.
[56] G. Bisio, L. Tagliafico, On the recovery of LNG physical exergy by means of a simple cycle or a complex system, Exergy, an International Journal 2 (2002) 34–50.
[57] L. Zheng, S. Zhang, B. Wang, L. Zhao, Y. Xiao, The Cooling Air and Firing Temperature Estimation for GE's Heavy Duty Gas Turbines, Proceedings of the Chinese Society of Electrical Engineering, 39 (2019) 6934-6943.
[58] J. Wang, Y. Gu, Parametric studies on different gas turbine cycles for a high temperature gas-cooled reactor, Nucl. Eng. Des. 235 (2005) 1761–1772.
[59] R. Scaccabarozzi, M. Gatti, E. Martelli, Thermodynamic analysis and numerical optimization of the NET power oxy-combustion cycle, Appl. Energy 178 (2016) 505–526.
[60] Y. Zhao, B. Yu, B. Wang, S. Zhang, Y. Xiao, Heat integration and optimization of direct-fired supercritical CO2 power cycle coupled to coal gasification process, Appl. Therm. Eng. 130 (2018) 1022–1032.
[61] I.H. Kim, H.C. No, Physical model development and optimal design of PCHE for intermediate heat exchangers in HTGRs, Nucl. Eng. Des. 243 (2012) 243–250.
[62] M. Romero Gómez, J. Romero Gómez, L.M. López-González, L.M. López-Ochoa, Thermodynamic analysis of a novel power plant with LNG (liquefied natural gas) cold exergy exploitation and CO2 capture, Energy 105 (2016) 32–44.
[63] A. Mohamad, A. Haouam, C. Derbal, H. Mzad, J. Taler, A.C. Benim, R. Bennacer, S. H. Suh, R. de Lieto Vollaro, A. Vallati, G. Battista, Thermal performance of a gas turbine based on an exergy analysis, E3S Web of Conferences 128 (2019).
[64] T.K. Ibrahim, F. Basrawi, O.I. Awad, A.N. Abdullah, G. Najafi, R. Mamat, F. Y. Hagos, Thermal performance of gas turbine power plant based on exergy analysis, Appl. Therm. Eng. 115 (2017) 977–985.
[65] J.-Q. Guo, M.-J. Li, J.-L. Xu, J.-J. Yan, T. Ma, Energy, exergy and economic (3E) evaluation and conceptual design of the 1000 MW coal-fired power plants integrated with S-CO2 Brayton cycles, Energ. Conver. Manage. 211 (2020).
[66] S. Park, J. Kim, M. Yoon, D. Rhim, C. Yeom, Thermodynamic and economic investigation of coal-fired power plant combined with various supercritical CO2 Brayton power cycle, Appl. Therm. Eng. 130 (2018) 611–623.
[67] H. Ghaebi, M. Amidpour, S. Karimkashi, O. Rezayan, Energy, exergy and thermoeconomic analysis of a combined cooling, heating and power (CCHP) system with gas turbine prime mover, Int. J. Energy Res. 35 (2011) 697–709.
[68] M. Gorji-Bandpy, H. Goodarzian, M. Biglari, The cost-effective analysis of a gas turbine power plant, Energy Sources Part B-Economics Planning and Policy 5 (2010) 348–358.
[69] Z. Guo-Yan, W. En, T. Shan-Tung, Techno-economic study on compact heat exchangers, Int. J. Energy Res. 32 (2008) 1119–1127.
[70] D. Prakash, O. Singh, Thermo-economic study of combined cycle power plant with carbon capture and methanation, J. Clean. Prod. 231 (2019) 529–542.
[71] V. Zare, S.M.S. Mahmoudi, M. Yari, An exergoeconomic investigation of waste heat recovery from the gas turbine-Modular helium reactor (GT-MHR) employing an ammonia–water power/cooling cycle, Energy 61 (2013) 397–409.
[72] Z.G. Qu, Y.H. Bai, L. Pu, One-dimensional numerical study of thermal performance of an organic rankine cycle system using liquefied natural gas as a cold source for cold energy recovery, J. Nat. Gas Sci. Eng. 26 (2015) 1399–1413.
[73] M.H. Ahmadi, M. Mehrpooya, F. Pourfayaz, Exergoeconomic analysis and multi objective optimization of performance of a Carbon dioxide power cycle driven by geothermal energy with liquefied natural gas as its heat sink, Energ. Conver. Manage. 119 (2016) 422–434.
[74] Y. Liu, J. Han, H. You, Exergoeconomic analysis and multi-objective optimization of a CCHP system based on LNG cold energy utilization and flue gas waste heat recovery with CO2 capture, Energy 190 (2020) 116201.